European Conference on Computational Fluid Dynamics
ECCOMAS CFD 2006
P. Wesseling, E. Oñate and J. Périaux (Eds)


# A MONOLITHIC FEM SOLVER FOR AN ALE FORMULATION OF FLUID–STRUCTURE INTERACTION WITH CONFIGURATION FOR NUMERICAL BENCHMARKING

**Jaroslav Hron, Stefan Turek***

Institute of Applied Mathematics, LS III, University of Dortmund
Vogelpothsweg 87, 44227 Dortmund, Germany
e-mail: hron@math.uni-dortmund.de, turek@math.uni-dortmund.de

**Key words:** fluid-structure interaction, ALE, monolithic FEM

**Abstract.** *We investigate a monolithic algorithm to solve the problem of time dependent interaction between an incompressible viscous fluid and an elastic solid. The continuous formulation of the problem and its discretization is done in a monolithic way, treating the problem as one continuum. The $Q_2/P_1^{dis}$ finite elements are used for the discretization and an approximate Newton method with coupled multigrid linear solver is developed for solving the equations. We discuss possible efficient strategies of setting up the resulting system and its solution. A 2-dimensional configuration is presented to test the developed method. It is based on the older successful DFG benchmark* flow around cylinder *for incompressible laminar fluid flow. Similar to this older benchmark we consider the flow to be incompressible and in the laminar regime. The structure is allowed to be compressible or incompressible and the deformations of the structure are periodic and significant in terms of displacement. This configuration can be used to compare different numerical methods and code implementations for the fluid-structure interaction problem qualitatively and particularly quantitatively with respect to efficiency and accuracy of the computation.*

## 1 INTRODUCTION

We consider the problem of viscous fluid flow interacting with an elastic body which is being deformed by the fluid action. Such a problem is encountered in many real life applications of great importance. Typical examples of this type of problem are the areas of aero-elasticity, biomechanics or material processing. For example, a good mathematical model for biological tissue could be used in such areas as early recognition or prediction of heart muscle failure, advanced design of new treatments and operative procedures, and the understanding of atherosclerosis and associated problems. Other possible applications

*This work has been supported by German Reasearch Association (DFG), Reasearch unit 493.

include the development of virtual reality programs for training new surgeons or designing new operative procedures[8].

### 1.1 Theoretical results

The theoretical investigation of fluid structure interaction problems is complicated by the need of mixed description. While for the solid part the natural view is the material (Lagrangian) description, for the fluid it is the spatial (Eulerian) description. In the case of their combination some kind of mixed description (usually referred to as the arbitrary Lagrangian-Eulerian description or ALE) has to be used which brings additional nonlinearity into the resulting equations. In[7] a time dependent, linearized model of interaction between a viscous fluid and an elastic shell in small displacement approximation and its discretization is analyzed. The problem is further simplified by neglecting all changes in the geometry configuration. Under these simplifications by using energy estimates they are able to show that the proposed formulation is well posed and a global weak solution exists. Further they show that an independent discretization by standard mixed finite elements for the fluid and by nonconforming discrete Kirchhoff triangle finite elements for the shell together with backward or central difference approximation of the time derivatives converges to the solution of the continuous problem.

In[9] a steady problem of equilibrium of an elastic fixed obstacle surrounded by a viscous fluid is studied. Existence of an equilibrium state is shown with the displacement and velocity in $C^{2,\alpha}$ and pressure in $C^{1,\alpha}$ under assumption of small data in $C^{2,\alpha}$ and domain boundaries of class $C^3$.

A numerical solution of the resulting equations of the fluid structure interaction problem poses a great challenge since it includes the features of nonlinear elasticity, fluid mechanics and their coupling. The easiest solution strategy, mostly used in the available software packages, is to decouple the problem into the fluid part and solid part, for each of those parts to use some well established method of solution then the interaction is introduced as external boundary conditions in each of the subproblems. This has an advantage that there are many well tested finite element based numerical methods for separate problems of fluid flow and elastic deformation, on the other hand the treatment of the interface and the interaction is problematic. The approach presented here treats the problem as a single continuum with the coupling automatically taken care of as internal interface, which in our formulation does not require any special treatment.

## 2 CONTINUUM DESCRIPTION

Let $\Omega \subset \mathbb{R}^3$ be a reference configuration of a given body. Let $\Omega_t \subset \mathbb{R}^3$ be a configuration of this body at time $t$. Then a one-to-one, sufficiently smooth mapping $\vec{\chi}_\Omega$ of the reference configuration $\Omega$ to the current configuration

$$\vec{\chi}_\Omega : \Omega \times [0,T] \mapsto \mathbb{R}^3, \tag{1}$$

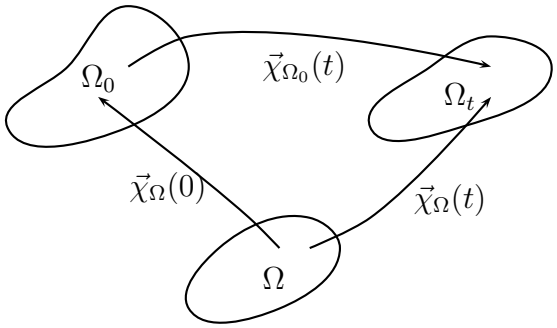


Figure 1: The referential domain $\Omega$, initial $\Omega_0$ and current state $\Omega_t$ and relations between them. The identification $\Omega \equiv \Omega_0$ is adopted in this text.

describes the motion of the body, see figure 1. The mapping $\vec{\chi}_\Omega$ depends on the choice of the reference configuration $\Omega$ which can be fixed in a various ways. Here we think of $\Omega$ to be the initial (stress-free) configuration $\Omega_0$. Thus, if not emphasized, we mean by $\vec{\chi}$ exactly $\vec{\chi}_\Omega = \vec{\chi}_{\Omega_0}$. If we denote by $\vec{X}$ a material point in the reference configuration $\Omega$ then the position of this point at time $t$ is given by

$$\vec{x} = \vec{\chi}(\vec{X}, t). \tag{2}$$

Next, the mechanical fields describing the deformation are defined in a standard manner. The displacement field, the velocity field, deformation gradient and its determinant are

$$\vec{u}(\vec{X}, t) = \vec{\chi}(\vec{X}, t) - \vec{X}, \qquad \vec{v} = \frac{\partial \vec{\chi}}{\partial t}, \qquad \boldsymbol{F} = \frac{\partial \vec{\chi}}{\partial \vec{X}}, \qquad J = \det \boldsymbol{F}. \tag{3}$$

Let us adopt the following useful notations for some derivatives. Any field quantity $\varphi$ with values in some vector space $Y$ (i.e. scalar, vector or tensor valued) can be expressed in the Eulerian description as a function of the spatial position $\vec{x} \in \mathbb{R}^3$

$$\varphi = \tilde{\varphi}(\vec{x}, t) : \Omega_t \times [0, T] \mapsto Y.$$

Then we define following notations for the derivatives of the field $\varphi$

$$\frac{\partial \varphi}{\partial t} := \frac{\partial \tilde{\varphi}}{\partial t}, \qquad \nabla \varphi = \frac{\partial \varphi}{\partial \vec{x}} := \frac{\partial \tilde{\varphi}}{\partial \vec{x}}, \qquad \operatorname{div} \varphi := \operatorname{tr} \nabla \varphi. \tag{4}$$

In the case of Lagrangian description we consider the quantity $\varphi$ to be defined on the reference configuration $\Omega$, then for any $\vec{X} \in \Omega$ we can express the quantity $\varphi$ as

$$\varphi = \bar{\varphi}(\vec{X}, t) : \Omega \times [0, T] \mapsto Y,$$

and we define the derivatives of the field $\varphi$ as

$$\frac{d \varphi}{dt} := \frac{\partial \bar{\varphi}}{\partial t}, \qquad \operatorname{Grad} \varphi = \frac{\partial \varphi}{\partial \vec{X}} := \frac{\partial \bar{\varphi}}{\partial \vec{X}}, \qquad \operatorname{Div} \varphi := \operatorname{tr} \operatorname{Grad} \varphi. \tag{5}$$

These two descriptions can be related to each other through following relations

$$\bar{\varphi}(\vec{X},t) = \tilde{\varphi}(\vec{\chi}(\vec{X},t),t), \tag{6}$$

$$\frac{d\varphi}{dt} = \frac{\partial\varphi}{\partial t} + (\nabla\varphi)\vec{v}, \qquad \operatorname{Grad}\varphi = (\nabla\varphi)\boldsymbol{F}, \qquad \int_{\Omega_t}\varphi dv = \int_{\Omega}\varphi J dV \tag{7}$$

$$\frac{d\boldsymbol{F}}{dt} = \operatorname{Grad}\vec{v}, \qquad \frac{\partial J}{\partial \boldsymbol{F}} = J\boldsymbol{F}^{-T}, \qquad \frac{dJ}{dt} = J\operatorname{div}\vec{v}. \tag{8}$$

For the formulation of the balance laws we will need to express a time derivatives of some integrals. The following series of equalities obtained by using the previously stated relations will be useful

$$\begin{aligned}\frac{d}{dt}\int_{\Omega_t}\varphi dv &= \frac{d}{dt}\int_{\Omega}\varphi J dV = \int_{\Omega}\frac{d}{dt}(\varphi J)\,dV = \int_{\Omega_t}\left(\frac{d\varphi}{dt} + \varphi\operatorname{div}\vec{v}\right)dv \\ &= \int_{\Omega_t}\left(\frac{\partial\varphi}{\partial t} + \operatorname{div}(\varphi\vec{v})\right)dv = \int_{\Omega_t}\frac{\partial\varphi}{\partial t}dv + \int_{\partial\Omega_t}\varphi\vec{v}\cdot\vec{n}da \\ &= \frac{\partial}{\partial t}\int_{\Omega_t}\varphi dv + \int_{\partial\Omega_t}\varphi\vec{v}\cdot\vec{n}da.\end{aligned} \tag{9}$$

The Piola identity is used, $\operatorname{Div}(J\boldsymbol{F}^{-T}) = \vec{0}$, which can be checked by differentiating the left hand side and using (8) together with an identity obtained by differentiating the relation $\boldsymbol{F}\boldsymbol{F}^{-1} = \boldsymbol{I}$.

### 2.1 Balance laws in the ALE formulation

The Eulerian (or spatial) description is well suited for a problem of fluid flowing through some spatially fixed region. In such a case the material particles can enter and leave the region of interest. The fundamental quantity describing the motion is the velocity vector. On the other hand the Lagrangian (or referential) description is well suited for a problem of deforming a given body consisting of a fixed set of material particles. In this case the actual boundary of the body can change its shape. The fundamental quantity describing the motion in this case is the vector of displacement from the referential state.

In the case of fluid-structure interaction problems we can still use the Lagrangian description for the deformation of the solid part. The fluid flow now takes place in a domain with boundary given by the deformation of the structure which can change in time and is influenced back by the fluid flow. The mixed ALE description of the fluid has to be used in this case. The fundamental quantity describing the motion of the fluid is still the velocity vector but the description is accompanied by a certain displacement field which describes the change of the fluid domain. This displacement field has no connection to the fluid velocity field and the purpose of its introduction is to provide a transformation of the current fluid domain and corresponding governing equations to some fixed reference domain. This method is sometimes called a pseudo-solid mapping method[10].

Let $\mathcal{P} \subset \mathbb{R}^3$ be a fixed region in space (a control volume) with the boundary $\partial\mathcal{P}$ and unit outward normal vector $\vec{n}_{\mathcal{P}}$, such that $\mathcal{P} \subset \Omega_t \quad$ for all $t \in [0,T]$. Let $\varrho$ denote the mass density of the material. Then the balance of mass in the region $\mathcal{P}$ can be written as

$$\frac{\partial}{\partial t}\int_{\mathcal{P}} \varrho dv + \int_{\partial\mathcal{P}} \varrho\vec{v}\cdot\vec{n}_{\mathcal{P}} da = 0. \tag{10}$$

If all the fields are sufficiently smooth this equation can be written in local form with respect to the current configuration as

$$\frac{\partial\varrho}{\partial t} + \operatorname{div}(\varrho\vec{v}) = 0. \tag{11}$$

It will be useful to derive the mass balance equation from the Lagrangian point of view. Let $\mathcal{Q} \subset \Omega$ be a fixed set of particles. Then $\vec{\chi}(\mathcal{Q},t) \subset \Omega_t$ is a region occupied by these particles at the time $t$, and the balance of mass can be expressed as

$$\frac{d}{dt}\int_{\vec{\chi}(\mathcal{Q},t)} \varrho dv = 0, \tag{12}$$

which in local form w.r.t. the reference configuration can be written as

$$\frac{d}{dt}(\varrho J) = 0. \tag{13}$$

In the case of an arbitrary Lagrangian-Eulerian description we take a region $\mathcal{Z} \subset \mathbb{R}^3$ which is itself moving independently of the motion of the body. Let the motion of the control region $\mathcal{Z}$ be described by a given mapping

$$\vec{\zeta}_{\mathcal{Z}} : \mathcal{Z}\times[0,T] \mapsto \mathbb{R}^3, \qquad \mathcal{Z}_t \subset \Omega_t \quad \forall t \in [0,T],$$

with the corresponding velocity $\vec{v}_{\mathcal{Z}} = \frac{\partial\vec{\zeta}_{\mathcal{Z}}}{\partial t}$, deformation gradient $\boldsymbol{F}_{\mathcal{Z}} = \frac{\partial\vec{\zeta}_{\mathcal{Z}}}{\partial\vec{X}}$ and its determinant $J_{\mathcal{Z}} = \det\boldsymbol{F}_{\mathcal{Z}}$. The mass balance equation can be written as

$$\frac{\partial}{\partial t}\int_{\mathcal{Z}_t} \varrho dv + \int_{\partial\mathcal{Z}_t} \varrho(\vec{v}-\vec{v}_{\mathcal{Z}})\cdot\vec{n}_{\mathcal{Z}_t} da = 0, \tag{14}$$

this can be viewed as an Eulerian description with a moving spatial coordinate system or as a grid deformation in the context of the finite element method. In order to obtain a local form of the balance relation we need to transform the integration to the fixed spatial region $\mathcal{Z}$

$$\frac{\partial}{\partial t}\int_{\mathcal{Z}} \varrho J_{\mathcal{Z}} dv + \int_{\partial\mathcal{Z}} \varrho(\vec{v}-\vec{v}_{\mathcal{Z}})\cdot\boldsymbol{F}_{\mathcal{Z}}^{-T}\vec{n}_{\mathcal{Z}} J_{\mathcal{Z}} da = 0, \tag{15}$$

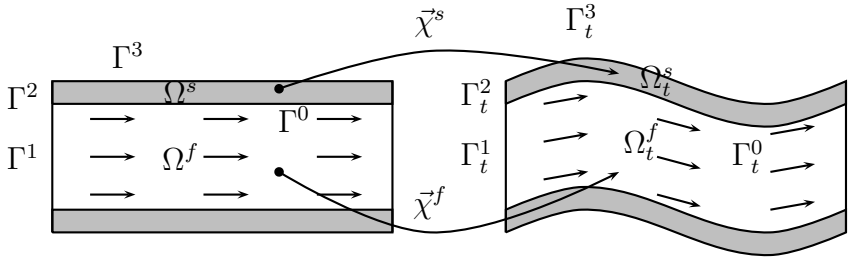


Figure 2: Undeformed (original) and deformed (current) configurations.

then the local form is

$$\frac{\partial}{\partial t}\left(\varrho J_{\mathcal{Z}}\right) + \operatorname{div}\left(\varrho J_{\mathcal{Z}}(\vec{v} - \vec{v}_{\mathcal{Z}}) \cdot \boldsymbol{F}_{\mathcal{Z}}^{-T}\right) = 0. \tag{16}$$

The two previous special formulations can be now recovered. If the region $\mathcal{Z}$ is not moving in space, i.e. $\mathcal{Z} = \mathcal{Z}_t, \forall t \in [0,T]$, then $\vec{\zeta}_{\mathcal{Z}}$ is the identity mapping, $\boldsymbol{F}_{\mathcal{Z}} = \boldsymbol{I}, J_{\mathcal{Z}} = 1, \vec{v}_{\mathcal{Z}} = \vec{0}$ and (16) reduces to (11). If the region $\mathcal{Z}$ moves exactly with the material, i.e. $\vec{\zeta}_{\mathcal{Z}} = \vec{\chi}|_{\mathcal{Z}}$ then $\boldsymbol{F}_{\mathcal{Z}} = \boldsymbol{F}, J_{\mathcal{Z}} = J, \vec{v}_{\mathcal{Z}} = \vec{v}$ and (16) reduces to (13).

The balance of linear momentum in ALE formulation is obtained in a similar way and the details can be found in[5].

## 3 FLUID STRUCTURE INTERACTION PROBLEM FORMULATION

At this point we make a few assumptions that allow us to deal with the task of setting up a tractable problem. Let us consider a flow between thick elastic walls as shown in figure 2. We will use the superscripts $^s$ and $^f$ to denote the quantities connected with the solid and fluid. Let us assume that both materials are incompressible and all the processes are isothermal, which is a well accepted approximation in biomechanics, and let us denote the constant densities of each material by $\varrho^f, \varrho^s$.

### 3.1 Monolithic description

We denote by $\Omega_t^f$ the domain occupied by the fluid and $\Omega_t^s$ by the solid at time $t \in [0,T]$. Let $\Gamma_t^0 = \bar{\Omega}_t^f \cap \bar{\Omega}_t^s$ be the part of the boundary where the solid interacts with the fluid and $\Gamma_t^i, i = 1,2,3$ be the remaining external boundaries of the solid and the fluid as depicted in figure 2.

Let the deformation of the solid part be described by the mapping $\vec{\chi}^s$

$$\vec{\chi}^s : \Omega^s \times [0,T] \mapsto \mathbb{R}^3, \tag{17}$$

with the corresponding displacement $\vec{u}^s$ and the velocity $\vec{v}^s$ given by

$$\vec{u}^s(\vec{X},t) = \vec{\chi}^s(\vec{X},t) - \vec{X}, \qquad \vec{v}^s(\vec{X},t) = \frac{\partial \vec{\chi}^s}{\partial t}(\vec{X},t). \tag{18}$$

The fluid flow is described by the velocity field $\vec{v}^f$ defined on the fluid domain $\Omega_t^f$

$$\vec{v}^f(\vec{x},t) : \Omega_t^f \times [0,T] \mapsto \mathbb{R}^3. \tag{19}$$

Further we define the auxiliary mapping, denoted by $\vec{\zeta}^f$, to describe the change of the fluid domain and corresponding displacement $\vec{u}^f$ by

$$\vec{\zeta}^f : \Omega^f \times [0,T] \mapsto \mathbb{R}^3, \qquad \vec{u}^f(\vec{X},t) = \vec{\zeta}^f(\vec{X},t) - \vec{X}. \tag{20}$$

We require that the mapping $\vec{\zeta}^f$ is sufficiently smooth, one to one and has to satisfy

$$\vec{\zeta}^f(\vec{X},t) = \vec{\chi}^s(\vec{X},t), \quad \forall(\vec{X},t) \in \Gamma^0 \times [0,T]. \tag{21}$$

In the context of the finite element method this will describe the artificial mesh deformation inside the fluid region and it will be constructed as a solution to a suitable boundary value problem with (21) as the boundary condition.

The momentum and mass balance of the fluid in the time dependent fluid domain analogous to (16) are

$$\varrho^f \frac{\partial \vec{v}^f}{\partial t} + \varrho^f (\nabla \vec{v}^f)(\vec{v}^f - \frac{\partial \vec{u}^f}{\partial t}) = \operatorname{div} \boldsymbol{\sigma}^f, \qquad \operatorname{div} \vec{v}^f = 0 \qquad \text{in } \Omega^f_t, \tag{22}$$

together with the momentum and mass balance of the solid in the solid domain

$$\varrho^s \frac{\partial \vec{v}^s}{\partial t} + \varrho^s (\nabla \vec{v}^s)\vec{v}^s = \operatorname{div} \boldsymbol{\sigma}^s, \qquad \operatorname{div} \vec{v}^s = 0 \qquad \text{in } \Omega^s_t. \tag{23}$$

The interaction is due to the exchange of momentum through the common part of the boundary $\Gamma^0_t$. On this part we require that the forces are in balance and simultaneously the no slip boundary condition holds for the fluid, i.e.

$$\boldsymbol{\sigma}^f \vec{n} = \boldsymbol{\sigma}^s \vec{n} \quad \text{ on } \Gamma^0_t, \qquad \vec{v}^f = \vec{v}^s \quad \text{ on } \Gamma^0_t. \tag{24}$$

The remaining external boundary conditions can be of the following kind. A natural boundary condition on the fluid inflow and outflow part $\Gamma^1_t$ with $p_B$ given value. Alternatively we can prescribe a Dirichlet type boundary condition on the inflow or outflow part $\Gamma^1_t$

$$\boldsymbol{\sigma}^f \vec{n} = p_B \vec{n} \quad \text{ on } \Gamma^1_t, \qquad \vec{v}^f = \vec{v}_B \quad \text{ on } \Gamma^1_t, \tag{25}$$

where $\vec{v}_B$ is given. The Dirichlet boundary condition is prescribed for the solid displacement at the part $\Gamma^2_t$ and the stress free boundary condition for the solid is applied at the part $\Gamma^3_t$

$$\vec{u}^s = \vec{0} \quad \text{ on } \Gamma^2_t, \qquad \boldsymbol{\sigma}^s \vec{n} = \vec{0} \quad \text{ on } \Gamma^3_t. \tag{26}$$

We introduce the domain $\Omega = \Omega^f \cup \Omega^s$, where $\Omega^f, \Omega^s$ are the domains occupied by the fluid and solid in the initial undeformed state, and two fields defined on this domain as

$$\vec{u} : \Omega \times [0,T] \to \mathbb{R}^3, \qquad \vec{v} : \Omega \times [0,T] \to \mathbb{R}^3,$$

such that the field $\vec{v}$ represents the velocity at the given point and $\vec{u}$ the displacement on the solid part and the artificial displacement in the fluid part, taking care of the fact that the fluid domain is changing with time,

$$\vec{v} = \begin{cases} \vec{v}^s & \text{on } \Omega^s, \\ \vec{v}^f & \text{on } \Omega^f, \end{cases} \qquad \vec{u} = \begin{cases} \vec{u}^s & \text{on } \Omega^s, \\ \vec{u}^f & \text{on } \Omega^f. \end{cases} \tag{27}$$

Due to the conditions (21) and (24) both fields are continuous across the interface $\Gamma_t^0$ and we can define global quantities on $\Omega$ as the deformation gradient and its determinant

$$\boldsymbol{F} = \boldsymbol{I} + \operatorname{Grad} \vec{u}, \qquad J = \det \boldsymbol{F}. \tag{28}$$

Using this notation the solid balance laws (23) can be expressed in the Lagrangian formulation with the initial configuration $\Omega^s$ as reference,

$$J\varrho^s \frac{d\vec{v}}{dt} = \operatorname{Div} \boldsymbol{P}^s, \qquad J = 1 \qquad \text{in } \Omega^s. \tag{29}$$

The fluid equations (22) are already expressed in the arbitrary Lagrangian-Eulerian formulation with respect to the time dependent region $\Omega_t^f$, now we transform the equations to the fixed initial region $\Omega^f$ by the mapping $\zeta^f$ defined by (20)

$$\varrho^f \frac{\partial \vec{v}}{\partial t} + \varrho^f (\operatorname{Grad} \vec{v}) \boldsymbol{F}^{-1} (\vec{v} - \frac{\partial \vec{u}}{\partial t}) = J^{-1} \operatorname{Div}(J \boldsymbol{\sigma}^f F^{-T}), \quad \operatorname{Div}(J \vec{v} \boldsymbol{F}^{-T}) = 0 \quad \text{in } \Omega^f. \tag{30}$$

It remains to prescribe some relation for the mapping $\zeta^f$. In terms of the corresponding displacement $\vec{u}^f$ we formulate some simple relation together with the Dirichlet boundary conditions required by (21), for example

$$\frac{\partial \vec{u}}{\partial t} = \Delta \vec{u} \quad \text{in } \Omega^f, \qquad \vec{u} = \vec{u}^s \quad \text{on } \Gamma^0, \qquad \vec{u} = \vec{0} \quad \text{on } \Gamma^1. \tag{31}$$

Other choices are possible. For example, the mapping $\vec{u}^f$ can be realized as a solution of the elasticity problem with the same Dirichlet boundary conditions[10].

The complete set of the equations can be written as

$$\frac{\partial \vec{u}}{\partial t} = \begin{cases} \vec{v} & \text{in } \Omega^s, \\ \Delta \vec{u} & \text{in } \Omega^f, \end{cases} \tag{32}$$

$$\frac{\partial \vec{v}}{\partial t} = \begin{cases} \frac{1}{J\varrho^s} \operatorname{Div} \boldsymbol{P}^s & \text{in } \Omega^s, \\ -(\operatorname{Grad} \vec{v}) \boldsymbol{F}^{-1} (\vec{v} - \frac{\partial \vec{u}}{\partial t}) + \frac{1}{J\varrho^f} \operatorname{Div}(J \boldsymbol{\sigma}^f \boldsymbol{F}^{-T}) & \text{in } \Omega^f, \end{cases} \tag{33}$$

$$0 = \begin{cases} J - 1 & \text{in } \Omega^s, \\ \operatorname{Div}(J \vec{v} \boldsymbol{F}^{-T}) & \text{in } \Omega^f, \end{cases} \tag{34}$$

with the initial conditions

$$\vec{u}(0) = \vec{0} \quad \text{in } \Omega, \qquad \vec{v}(0) = \vec{v}_0 \quad \text{in } \Omega, \tag{35}$$

and boundary conditions

$$\vec{u} = \vec{0}, \quad \vec{v} = \vec{v}_B \quad \text{on } \Gamma^1, \qquad \vec{u} = \vec{0} \quad \text{on } \Gamma^2, \qquad \boldsymbol{\sigma}^s \vec{n} = \vec{0} \quad \text{on } \Gamma^3. \tag{36}$$

### 3.2 Constitutive equations

In order to solve the balance equations we need to specify the constitutive relations for the stress tensors. For the fluid we use the incompressible Newtonian relation

$$\boldsymbol{\sigma}^f = -p^f \boldsymbol{I} + \mu(\nabla \vec{v}^f + (\nabla \vec{v}^f)^T), \tag{37}$$

where $\mu$ represents the viscosity of the fluid and $p^f$ is the Lagrange multiplier corresponding to the incompressibility constraint.

For the solid part we assume that it can be described by an incompressible hyper-elastic material. We specify the Helmholtz potential $\Psi$ and the solid Cauchy stress tensor and the first Piola-Kirchhoff stress tensor are given by

$$\boldsymbol{\sigma}^s = -p^s \boldsymbol{I} + \varrho^s \frac{\partial \Psi}{\partial \boldsymbol{F}} \boldsymbol{F}^T, \qquad \boldsymbol{P}^s = -J p^s \boldsymbol{F}^{-T} + J \varrho^s \frac{\partial \Psi}{\partial \boldsymbol{F}}, \tag{38}$$

where $p^s$ is the Lagrange multiplier corresponding to the incompressibility constraint.

Then the material is specified by prescribing the Helmholtz potential as a function of the deformation

$$\Psi = \hat{\Psi}(\boldsymbol{F}) = \tilde{\Psi}(\boldsymbol{C}), \tag{39}$$

where $\boldsymbol{C} = \boldsymbol{F}^T \boldsymbol{F}$ is the right Cauchy-Green deformation tensor. Typical examples for the Helmholtz potential used for isotropic materials like rubber is the Mooney-Rivlin material

$$\tilde{\Psi} = c_1(I_C - 3) + c_2(II_C - 3), \tag{40}$$

where $I_C = \operatorname{tr} \boldsymbol{C}, II_C = \operatorname{tr} \boldsymbol{C}^2 - \operatorname{tr}^2 \boldsymbol{C}, III_C = \det \boldsymbol{C}$ are the invariants of the right Cauchy-Green deformation tensor $\boldsymbol{C}$ and $c_i$ are some material constants. A special case of neo-Hookean material is obtained for $c_2 = 0$. With a suitable choice of the material parameters the entropy inequality and the balance of energy are automatically satisfied.

### 3.3 Weak formulation

We non-dimensionalize all the quantities by a given characteristic length $L$ and speed $V$ as follows

$$\hat{t} = t\frac{V}{L}, \qquad \hat{\vec{x}} = \frac{\vec{x}}{L}, \qquad \hat{\vec{u}} = \frac{\vec{u}}{L}, \qquad \hat{\vec{v}} = \frac{\vec{v}}{V},$$
$$\hat{\boldsymbol{\sigma}}^s = \boldsymbol{\sigma}^s \frac{L}{\varrho^f V^2}, \qquad \hat{\boldsymbol{\sigma}}^f = \boldsymbol{\sigma}^f \frac{L}{\varrho^f V^2}, \qquad \hat{\mu} = \frac{\mu}{\varrho^f V L}, \qquad \hat{\Psi} = \Psi \frac{L}{\varrho^f V^2},$$

further using the same symbols, without the hat, for the non-dimensional quantities. The non-dimensionalized system with the choice of material relations, (37) for viscous fluid and (38) for the hyper-elastic solid is

$$\frac{\partial \vec{u}}{\partial t} = \begin{cases} \vec{v} & \text{in } \Omega^s, \\ \Delta \vec{u} & \text{in } \Omega^f, \end{cases} \tag{41}$$

$$\frac{\partial \vec{v}}{\partial t} = \begin{cases} \frac{1}{\beta} \operatorname{Div}\left(-Jp^s \boldsymbol{F}^{-T} + \frac{\partial \Psi}{\partial \boldsymbol{F}}\right) & \text{in } \Omega^s, \\ -(\operatorname{Grad} \vec{v})\boldsymbol{F}^{-1}(\vec{v} - \frac{\partial \vec{u}}{\partial t}) & \\ \quad + \operatorname{Div}\left(-Jp^f \boldsymbol{F}^{-T} + J\mu \operatorname{Grad} \vec{v}\boldsymbol{F}^{-1}\boldsymbol{F}^{-T}\right) & \text{in } \Omega^f, \end{cases} \tag{42}$$

$$0 = \begin{cases} J - 1 & \text{in } \Omega^s, \\ \operatorname{Div}(J\vec{v}\boldsymbol{F}^{-T}) & \text{in } \Omega^f, \end{cases} \tag{43}$$

and the boundary conditions

$$\boldsymbol{\sigma}^f \vec{n} = \boldsymbol{\sigma}^s \vec{n} \quad \text{on } \Gamma_t^0, \qquad \vec{v} = \vec{v}_B \quad \text{on } \Gamma_t^1, \tag{44}$$

$$\vec{u} = \vec{0} \quad \text{on } \Gamma_t^2, \qquad \boldsymbol{\sigma}^f \vec{n} = \vec{0} \quad \text{on } \Gamma_t^3. \tag{45}$$

Let $I = [0, T]$ denote the time interval of interest. We multiply the equations (41)-(43) by the test functions $\vec{\zeta}, \vec{\xi}, \gamma$ such that $\vec{\zeta} = \vec{0}$ on $\Gamma^2$, $\vec{\xi} = \vec{0}$ on $\Gamma^1$ and integrate over the space domain $\Omega$ and the time interval $I$. Using integration by parts on some of the terms and the boundary conditions we obtain

$$\int_0^T \int_\Omega \frac{\partial \vec{u}}{\partial t} \cdot \vec{\zeta} dV dt = \int_0^T \int_{\Omega^s} \vec{v} \cdot \vec{\zeta} dV dt - \int_0^T \int_{\Omega^f} \operatorname{Grad} \vec{u} \cdot \operatorname{Grad} \vec{\zeta} dV dt, \tag{46}$$

$$\begin{aligned} &\int_0^T \int_{\Omega^f} J \frac{\partial \vec{v}}{\partial t} \cdot \vec{\xi} dV dt + \int_0^T \int_{\Omega^s} \beta J \frac{\partial \vec{v}}{\partial t} \cdot \vec{\xi} dV dt \\ &\quad + \int_0^T \int_{\Omega^f} J \operatorname{Grad} \vec{v}\boldsymbol{F}^{-1}(\vec{v} - \frac{\partial \vec{u}}{\partial t}) \cdot \vec{\xi} dV dt - \int_0^T \int_\Omega Jp\boldsymbol{F}^{-T} \cdot \operatorname{Grad} \vec{\xi} dV dt \\ &\quad + \int_0^T \int_{\Omega^s} \frac{\partial \Psi}{\partial \boldsymbol{F}} \cdot \operatorname{Grad} \vec{\xi} dV dt + \int_0^T \int_{\Omega^f} J\mu \operatorname{Grad} \vec{v}\boldsymbol{F}^{-1}\boldsymbol{F}^{-T} \cdot \operatorname{Grad} \vec{\xi} dV dt = 0, \end{aligned} \tag{47}$$

$$\int_0^T \int_{\Omega^s} (J - 1)\gamma dV dt + \int_0^T \int_{\Omega^f} \operatorname{Div}(J\vec{v}\boldsymbol{F}^{-T})\gamma dV dt = 0. \tag{48}$$

Let us define the following spaces

$$\begin{aligned} U &= \{\vec{u} \in L^\infty(I, [W^{1,2}(\Omega)]^3), \vec{u} = \vec{0} \text{ on } \Gamma^2\}, \\ V &= \{\vec{v} \in L^2(I, [W^{1,2}(\Omega_t)]^3) \cap L^\infty(I, [L^2(\Omega_t)]^3), \vec{v} = \vec{0} \text{ on } \Gamma^1\}, \\ P &= \{p \in L^2(I, L^2(\Omega))\}, \end{aligned}$$

then the variational formulation of the fluid-structure interaction problem is to find $(\vec{u}, \vec{v} - \vec{v}_B, p) \in U \times V \times P$ such that equations (46), (47) and (48) are satisfied for all $(\vec{\zeta}, \vec{\xi}, \gamma) \in U \times V \times P$ including appropriate initial conditions.

### 3.4 Discretization

In the following, we restrict ourselves to two dimensions which allows systematic tests of the proposed methods in a very efficient way, particularly in view of grid-independent solutions. The time discretization is done by the Crank-Nicholson scheme which is only conditionally stable but which has better conservation properties than for example the implicit Euler scheme[4,6]. The Crank-Nicholson scheme can be obtained by dividing the time interval $I$ into the series of time steps $[t^n, t^{n+1}]$ with step length $k_n = t^{n+1} - t^n$. Assuming that the test functions are piecewise constant on each time step $[t^n, t^{n+1}]$, writing the weak formulation (46)-(47) for the time interval $[t^n, t^{n+1}]$, approximating the time derivatives by the central differences $\frac{\partial f}{\partial t} \approx \frac{f(t^{n+1}) - f(t^n)}{k_n}$ and approximating the time integration for the remaining terms by the trapezoidal quadrature rule as

$$\int_{t^n}^{t^{n+1}} f(t)dt \approx \frac{k_n}{2}(f(t^n) + f(t^{n+1})),$$

we obtain the time discretized system. The last equation corresponding to the incompressibility constraint is taken implicitly for the time $t^{n+1}$ and the corresponding term with the Lagrange multiplier $p_h^{n+1}$ in the equation (47) is also taken implicitly.

The discretization in space is done by the finite element method. We approximate the domain $\Omega$ by a domain $\Omega_h$ with polygonal boundary and by $\mathcal{T}_h$ we denote a set of quadrilaterals covering the domain $\Omega_h$. We assume that $\mathcal{T}_h$ is regular in the usual sense that any two quadrilateral are disjoint or have a common vertex or a common edge. By $\bar{T} = [-1, 1]^2$ we denote the reference quadrilateral. Our treatment of the problem as one system suggests that we use the same finite elements on both, the solid part and the fluid region. Since both materials are incompressible we have to choose a pair of finite element spaces known to be stable for the problems with incompressibility constraint. One possible choice is the conforming biquadratic, discontinuous linear $Q_2, P_1^{\text{dis}}$ pair, see figure 3 for the location of the degrees of freedom. This choice results in 39 degrees of freedom per element in the case of our displacement, velocity, pressure formulation in two dimensions and 112 degrees of freedom per element in three dimensions.

The spaces $U, V, P$ on an interval $[t^n, t^{n+1}]$ would be approximated in the case of the $Q_2, P_1^{\text{dis}}$ pair as

$$\begin{aligned}
U_h &= \{\vec{u}_h \in [C(\Omega_h)]^2, \vec{u}_h|_T \in [Q_2(T)]^2 \quad \forall T \in \mathcal{T}_h, \vec{u}_h = \vec{0} \text{ on } \Gamma_2\}, \\
V_h &= \{\vec{v}_h \in [C(\Omega_h)]^2, \vec{v}_h|_T \in [Q_2(T)]^2 \quad \forall T \in \mathcal{T}_h, \vec{v}_h = 0 \text{ on } \Gamma_1\}, \\
P_h &= \{p_h \in L^2(\Omega_h), p_h|_T \in P_1(T) \quad \forall T \in \mathcal{T}_h\}.
\end{aligned}$$

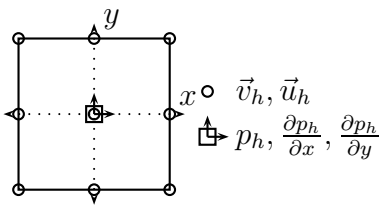


Figure 3: Location of the degrees of freedom for the $Q_2, P_1^{\text{dis}}$ element.

Let us denote by $\vec{u}_h^n$ the approximation of $\vec{u}(t^n)$, $\vec{v}_h^n$ the approximation of $\vec{v}(t^n)$ and $p_h^n$ the approximation of $p(t^n)$. Writing down the discrete equivalent of the equations (46)-(48) yields

$$\left(\vec{u}_h^{n+1} - \vec{u}_h^n, \vec{\eta}\right) - \frac{k_n}{2}\left\{ \left(\vec{v}_h^{n+1} + \vec{v}_h^n, \vec{\eta}\right)_s + \left(\nabla\vec{u}_h^{n+1} + \nabla\vec{u}_h^n, \nabla\vec{\eta}\right)_f \right\} = 0, \tag{49}$$

$$\begin{aligned}
&\left(J^{n+\frac{1}{2}}(\vec{v}_h^{n+1} - \vec{v}_h^n), \vec{\xi}\right)_f + \beta\left(\vec{v}_h^{n+1} - \vec{v}_h^n, \vec{\xi}\right)_s - k_n\left(J^{n+1}p_h^{n+1}(\boldsymbol{F}^{n+1})^{-T}, \operatorname{Grad}\vec{\xi}\right)_s \\
&+ \frac{k_n}{2}\Bigg\{ \left(\frac{\partial\Psi}{\partial\boldsymbol{F}}(\operatorname{Grad}\vec{u}_h^{n+1}), \operatorname{Grad}\vec{\xi}\right)_s + \left(J^{n+1}\operatorname{Grad}\vec{v}_h^{n+1}(\boldsymbol{F}^{n+1})^{-1}\vec{v}_h^{n+1}, \vec{\xi}\right)_f \\
&+ \mu\left(J^{n+1}\operatorname{Grad}\vec{v}_h^{n+1}(\boldsymbol{F}^{n+1})^{-1}, \operatorname{Grad}\vec{\xi}(\boldsymbol{F}^{n+1})^{-1}\right)_f \Bigg\} \\
&+ \frac{1}{2}\left((J^{n+1}\operatorname{Grad}\vec{v}_h^{n+1}(\boldsymbol{F}^{n+1})^{-1} + J^n\operatorname{Grad}\vec{v}_h^n(\boldsymbol{F}^n)^{-1})(\vec{u}_h^{n+1} - \vec{u}_h^n), \vec{\xi}\right)_f \\
&+ \frac{k_n}{2}\Bigg\{ \left(\frac{\partial\Psi}{\partial\boldsymbol{F}}(\operatorname{Grad}\vec{u}_h^n), \operatorname{Grad}\vec{\xi}\right)_s + \left(J^n\operatorname{Grad}\vec{v}_h^n(\boldsymbol{F}^n)^{-1}\vec{v}_h^n, \vec{\xi}\right)_f \\
&+ \mu\left(J^n\operatorname{Grad}\vec{v}_h^n(\boldsymbol{F}^n)^{-1}, \operatorname{Grad}\vec{\xi}(\boldsymbol{F}^n)^{-1}\right)_f \Bigg\} = 0,
\end{aligned} \tag{50}$$

$$\left(J^{n+1} - 1, \gamma\right)_s + \left(J^{n+1}\operatorname{Grad}\vec{v}_h^{n+1}(\boldsymbol{F}^{n+1})^{-1}, \gamma\right)_f = 0. \tag{51}$$

Using the basis of the spaces $U_h, V_h, P_h$ as the test functions $\vec{\zeta}, \vec{\xi}, \gamma$ we obtain a nonlinear algebraic set of equations. In each time step we have to find $\vec{X} = (\vec{u}_h^{n+1}, \vec{v}_h^{n+1}, p_h^{n+1}) \in U_h \times V_h \times P_h$ such that

$$\vec{\mathcal{F}}(\vec{X}) = \vec{0}, \tag{52}$$

where $\vec{\mathcal{F}}$ represents the discrete version of the system (49–51).

### 3.5 Solution algorithm

The system (52) of nonlinear algebraic equations is solved using Newton method as the basic iteration. One step of the Newton iteration can be written as

$$\vec{X}^{n+1} = \vec{X}^n - \left[\frac{\partial\vec{\mathcal{F}}}{\partial\vec{X}}(\vec{X}^n)\right]^{-1}\vec{\mathcal{F}}(\vec{X}^n). \tag{53}$$

1. Let $\vec{X}^n$ be some starting guess.
2. Set the residuum vector $\vec{R}^n = \vec{\mathcal{F}}(\vec{X}^n)$ and the tangent matrix $\boldsymbol{A} = \frac{\partial \vec{\mathcal{F}}}{\partial \vec{X}}(\vec{X}^n)$.
3. Solve for the correction $\delta\vec{X}$
$$\boldsymbol{A}\delta\vec{X} = \vec{R}^n.$$
4. Find optimal step length $\omega$.
5. Update the solution $\vec{X}^{n+1} = \vec{X}^n - \omega\delta\vec{X}$.

Figure 4: One step of the Newton method with the line search.

This basic iteration can exhibit quadratic convergence provided that the initial guess is sufficiently close to the solution. To ensure the convergence globally, some improvements of this basic iteration are used. The damped Newton method with line search improves the chance of convergence by adaptively changing the length of the correction vector. The solution update step in the Newton method (53) is replaced by $\vec{X}^{n+1} = \vec{X}^n + \omega\delta\vec{X}$, where the parameter $\omega$ is determined such that a certain error measure decreases. One of the possible choices for the quantity to decrease is

$$f(\omega) = \vec{\mathcal{F}}(\vec{X}^n + \omega\delta\vec{X}) \cdot \delta\vec{X}. \tag{54}$$

Since we know $f(0) = \vec{\mathcal{F}}(\vec{X}^n) \cdot \delta\vec{X}$, and $f'(0) = \left[\frac{\partial \vec{\mathcal{F}}}{\partial \vec{X}}(\vec{X}^n)\right] \delta\vec{X} \cdot \delta\vec{X} = \vec{\mathcal{F}}(\vec{X}^n) \cdot \delta\vec{X}$, computing $f(\omega_0)$ for $\omega_0 = -1$ or $\omega_0$ determined adaptively from previous iterations, we can approximate $f(\omega)$ by a quadratic function $f(\omega) = \frac{f(\omega_0) - f(0)(\omega_0+1)}{\omega_0^2}\omega^2 + f(0)(\omega + 1)$. Then setting $\tilde{\omega} = \frac{f(0)\omega_0^2}{f(\omega_0) - f(0)(\omega_0+1)}$, the new optimal step length $\omega \in [-1, 0]$ is

$$\omega = \begin{cases} -\dfrac{\tilde{\omega}}{2} & \text{if } \dfrac{f(0)}{f(\omega_0)} > 0, \\ -\dfrac{\tilde{\omega}}{2} - \sqrt{\dfrac{\tilde{\omega}^2}{4} - \tilde{\omega}} & \text{if } \dfrac{f(0)}{f(\omega_0)} \leq 0. \end{cases} \tag{55}$$

This line search can be repeated with $\omega_0$ taken as the last $\omega$ until, for example, $f(\omega) \leq \frac{1}{2}f(0)$. By this we can enforce a monotone convergence of the approximation $\vec{X}^n$.

An adaptive time-step selection was found to help in the nonlinear convergence. A heuristic algorithm was used to correct the time-step length according to the convergence of the nonlinear iterations in the previous time-step. If the convergence was close to quadratic, i.e. only up to three Newton steps were needed to obtain the required precision, the time step could be slightly increased, otherwise the time-step length was reduced.

The structure of the Jacobian matrix $\frac{\partial \vec{\mathcal{F}}}{\partial \vec{X}}$ is

$$\frac{\partial \vec{\mathcal{F}}}{\partial \vec{X}}(\vec{X}) = \begin{pmatrix} S_{uu} & S_{uv} & 0 \\ S_{vu} & S_{vv} & B_u + B_v \\ B_u^T & B_v^T & 0 \end{pmatrix}, \tag{56}$$

and it can be computed by finite differences from the residual vector $\vec{\mathcal{F}}(\vec{X})$

$$\left[\frac{\partial \vec{\mathcal{F}}}{\partial \vec{X}}\right]_{ij} (\vec{X}^n) \approx \frac{[\vec{\mathcal{F}}]_i(\vec{X}^n + \alpha_j \vec{e}_j) - [\vec{\mathcal{F}}]_i(\vec{X}^n - \alpha_j \vec{e}_j)}{2\alpha_j}, \tag{57}$$

where $\vec{e}_j$ are the unit basis vectors in $\mathbb{R}^n$ and the coefficients $\alpha_j$ are adaptively taken according to the change in the solution in the previous time step. Since we know the sparsity pattern of the Jacobian matrix in advance, it is given by the used finite element method, this computation can be done in an efficient way so that the linear solver remains the dominant part in terms of the CPU time. However, the resulting nonlinear and linear solution behavior is quite sensitive w.r.t. the parameters[5].

### 3.6 Multigrid solver

The solution of the linear problems is the most time consuming part of the solution process. A good candidate seems to be a direct solver for sparse systems like UMFPACK[3]; while this choice provides very robust linear solvers, its memory and CPU time requirements are too high for larger systems (i.e. more than 20000 unknowns). Large linear problems can be solved by Krylov space methods (BiCGStab, GMRes[1]) with suitable preconditioners. One possibility is the ILU preconditioner with special treatment of the saddle point character of our system, where we allow certain fill-in for the zero diagonal blocks[2]. The alternative option for larger systems is the multigrid method presented in this section.

We utilize the standard geometric multigrid approach based on a hierarchy of grids obtained by successive regular refinement of a given coarse mesh. The complete multigrid iteration is performed in the standard defect-correction setup with the V or F-type cycle. While a direct sparse solver[3] is used for the coarse grid solution, on finer levels a fixed number (2 or 4) of iterations by local MPSC schemes (Vanka-like smoother[11,14]) is performed. Such iteration can be written as

$$\begin{bmatrix} \vec{u}^{l+1} \\ \vec{v}^{l+1} \\ p^{l+1} \end{bmatrix} = \begin{bmatrix} \vec{u}^{l} \\ \vec{v}^{l} \\ p^{l} \end{bmatrix} - \omega \sum_{\text{Patch } \Omega_i} \begin{bmatrix} S_{\vec{u}\vec{u}|\Omega_i} & S_{\vec{u}\vec{v}|\Omega_i} & 0 \\ S_{\vec{v}\vec{u}|\Omega_i} & S_{\vec{v}\vec{v}|\Omega_i} & kB_{|\Omega_i} \\ c_{\vec{u}} B^T_{s|\Omega_i} & c_{\vec{v}} B^T_{f|\Omega_i} & 0 \end{bmatrix}^{-1} \begin{bmatrix} \mathbf{def}^l_{\vec{u}} \\ \mathbf{def}^l_{\vec{v}} \\ def^l_p \end{bmatrix}.$$

The inverse of the local systems ($39 \times 39$) can be done by hardware optimized direct solvers. The full nodal interpolation is used as the prolongation operator $\boldsymbol{P}$ with its transposed operator used as the restriction $\boldsymbol{R} = \boldsymbol{P}^T$.

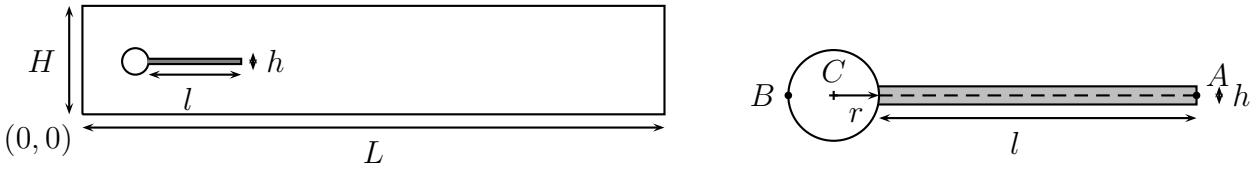


| | | value [m] |
|---|---|---|
| channel length | $L$ | 2.5 |
| channel width | $H$ | 0.41 |
| cylinder center position | $C$ | $(0.2, 0.2)$ |
| cylinder radius | $r$ | 0.05 |

| | | value [m] |
|---|---|---|
| elastic structure length | $l$ | 0.35 |
| elastic structure thickness | $h$ | 0.02 |
| reference point (at $t = 0$) | $A$ | $(0.6, 0.2)$ |
| reference point | $B$ | $(0.2, 0.2)$ |

Figure 5: Computational domain with the detail of the structure part.

## 4 BENCHMARK

For a rigorous evaluation of different methods for fluid-structure interaction problems we consider a benchmark proposed in[12]. The configurations consist of laminar incompressible channel flow around an elastic object which results in self-induced oscillations of the structure. Moreover, characteristic flow quantities and corresponding plots are provided for a quantitative comparison.

We consider the flow of an **incompressible Newtonian fluid** interacting with an **elastic solid**. We denote by $\Omega_t^f$ the domain occupied by the fluid and $\Omega_t^s$ by the solid at the time $t \in [0, T]$. Let $\Gamma_t^0 = \bar{\Omega}_t^f \cap \bar{\Omega}_t^s$ be the part of the boundary where the elastic solid interacts with the fluid. The fluid is considered to be **Newtonian**, **incompressible** and its state is described by the velocity and pressure fields $\vec{v}^f, p^f$. The constant density of the fluid is $\varrho^f$ and the viscosity is denoted by $\nu^f$. The Reynolds number is defined by $\mathrm{Re} = \frac{2r\bar{V}}{\nu^f}$, with the mean velocity $\bar{V} = \frac{2}{3}v(0, \frac{H}{2}, t)$, $r$ radius of the cylinder and $H$ height of the channel (see Fig. 5). The structure is assumed to be **elastic** and **compressible**. Its configuration is described by the displacement $\vec{u}^s$, with velocity field $\vec{v}^s = \frac{\partial \vec{u}^s}{\partial t}$. The material is specified by giving the Cauchy stress tensor $\boldsymbol{\sigma}^s$ (the 2nd Piola-Kirchhoff stress tensor is then given by $\boldsymbol{S}^s = J\boldsymbol{F}^{-1}\boldsymbol{\sigma}^s\boldsymbol{F}^{-T}$) by the following constitutive law for the **St. Venant-Kirchhoff** material ($\boldsymbol{E} = \frac{1}{2}(\boldsymbol{F}^{\mathrm{T}}\boldsymbol{F} - \boldsymbol{I})$)

$$\boldsymbol{\sigma}^s = \frac{1}{J}\boldsymbol{F}\left(\lambda^s(\mathrm{tr}\,\boldsymbol{E})\boldsymbol{I} + 2\mu^s\boldsymbol{E}\right)\boldsymbol{F}^{\mathrm{T}}, \qquad \boldsymbol{S}^s = \lambda^s(\mathrm{tr}\,\boldsymbol{E})\boldsymbol{I} + 2\mu^s\boldsymbol{E} \tag{58}$$

The boundary conditions on the fluid solid interface are assumed to be

$$\boldsymbol{\sigma}^f\vec{n} = \boldsymbol{\sigma}^s\vec{n}, \quad \vec{v}^f = \vec{v}^s \qquad \text{on } \Gamma_t^0, \tag{59}$$

where $\vec{n}$ is a unit normal vector to the interface $\Gamma_t^0$. This implies the no-slip condition for the flow, and that the forces on the interface are in balance.

The domain is based on the 2D version of the well-known CFD benchmark in[13] and shown here in figure 5. By omitting the elastic bar behind the cylinder one can exactly

| parameter | FSI1 | FSI2 | FSI3 |
|---|---|---|---|
| $\varrho^s$ $[10^3 \frac{\mathrm{kg}}{\mathrm{m}^3}]$ | 1 | 10 | 1 |
| $\nu^s$ | 0.4 | 0.4 | 0.4 |
| $\mu^s$ $[10^6 \frac{\mathrm{kg}}{\mathrm{ms}^2}]$ | 0.5 | 0.5 | 2.0 |
| $\varrho^f$ $[10^3 \frac{\mathrm{kg}}{\mathrm{m}^3}]$ | 1 | 1 | 1 |
| $\nu^f$ $[10^{-3} \frac{\mathrm{m}^2}{\mathrm{s}}]$ | 1 | 1 | 1 |
| $\bar{U}$ $[\frac{\mathrm{m}}{\mathrm{s}}]$ | 0.2 | 1 | 2 |

| parameter | FSI1 | FSI2 | FSI3 |
|---|---|---|---|
| $\beta = \frac{\varrho^s}{\varrho^f}$ | 1 | 10 | 1 |
| $\nu^s$ | 0.4 | 0.4 | 0.4 |
| $\mathrm{Ae} = \frac{E^s}{\varrho^f \bar{U}^2}$ | $3.5 \times 10^4$ | $1.4 \times 10^3$ | $1.4 \times 10^3$ |
| $\mathrm{Re} = \frac{\bar{U}d}{\nu^f}$ | 20 | 100 | 200 |
| $\bar{U}$ | 0.2 | 1 | 2 |

Table 1: Parameter settings for the full FSI benchmarks

recover the setup of the *flow around cylinder* configuration which allows for validation of the flow part by comparing the results with the older flow benchmark. The setting is intentionally non-symmetric[13] to prevent the dependence of the onset of any possible oscillation on the precision of the computation.

### 4.1 Boundary and initial conditions

A parabolic velocity profile is prescribed at the left channel inflow

$$v^f(0,y) = 1.5\bar{U}\frac{y(H-y)}{\left(\frac{H}{2}\right)^2} = 1.5\bar{U}\frac{4.0}{0.1681}y(0.41-y), \tag{60}$$

such that the mean inflow velocity is $\bar{U}$ and the maximum of the inflow velocity profile is $1.5\bar{U}$. The *no-slip* condition is prescribed for the fluid on the other boundary parts. i.e. top and bottom wall, circle and fluid-structure interface $\Gamma_t^0$.

The outflow condition can be chosen by the user, for example *stress free* or *do nothing* conditions. The outflow condition effectively prescribes some reference value for the pressure variable $p$. While this value could be arbitrarily set in the incompressible case, in the case of compressible structure this will have influence on the stress and consequently the deformation of the solid. In this proposal, we set the reference pressure at the outflow to have *zero mean value*.

Suggested starting procedure for the non-steady tests is to use a smooth increase of the velocity profile in time as

$$v^f(t,0,y) = \begin{cases} v^f(0,y)\frac{1-\cos(\frac{\pi}{2}t)}{2} & \text{if } t < 2.0 \\ v^f(0,y) & \text{otherwise} \end{cases} \tag{61}$$

where $v^f(0,y)$ is the velocity profile given in (60).

## 5 COMPUTATIONAL RESULTS

The mesh used for the computations is shown in Fig. 6. The following FSI tests are performed for two different inflow speeds. FSI1 is resulting in a steady state solution, while FSI2, FSI3 result in periodic solutions. The computed values are summarized in table 2 for the test FSI1 and in figures 7, 8 for the tests FSI2 and FSI3.

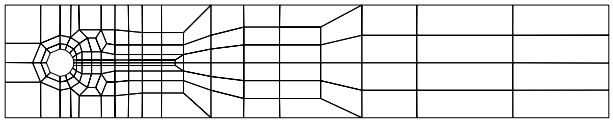

| level | #refine | #el | #dof |
|---|---|---|---|
| 0+0 | 0 | 62 | 1338 |
| 1+0 | 1 | 248 | 5032 |
| 2+0 | 2 | 992 | 19488 |
| 3+0 | 3 | 3968 | 76672 |
| 4+0 | 4 | 15872 | 304128 |

Figure 6: Example of a coarse mesh and the number of degrees of freedom for refined levels

| level | nel | ndof | ux of A $[\times 10^{-3}]$ | uy of A $[\times 10^{-3}]$ | drag | lift |
|---|---|---|---|---|---|---|
| $2+0$ | 992 | 19488 | 0.022871 | 0.81930 | 14.27360 | 0.76178 |
| $3+0$ | 3968 | 76672 | 0.022775 | 0.82043 | 14.29177 | 0.76305 |
| $4+0$ | 15872 | 304128 | 0.022732 | 0.82071 | 14.29484 | 0.76356 |
| $5+0$ | 63488 | 1211392 | 0.022716 | 0.82081 | 14.29486 | 0.76370 |
| $6+0$ | 253952 | 4835328 | 0.022708 | 0.82086 | 14.29451 | 0.76374 |
| **ref.** | | | 0.0227 | 0.8209 | 14.295 | 0.7638 |

Table 2: Results for **FSI1**

## 6 SUMMARY

In this contribution we presented a general formulation of dynamic fluid-structure interaction problems suitable for applications with finite deformations and laminar flows. While the presented example calculations are simplified to allow initial testing of the numerical methods[12] the formulation is general enough to allow immediate extension to more realistic material models.

To obtain the solution approximation the discrete systems resulting from the finite element discretization of the governing equations need to be solved which requires sophisticated solvers of nonlinear systems and fast solvers for very large linear systems which have to be further improved for full 3D problems and for more complicated models like visco-elastic materials for the fluid or solid components. The main advantage of the presented numerical method is its accuracy and robustness with respect to the constitutive models. Possible directions of increasing the efficiency of the solvers include the development of improved multigrid solvers, for instance of global pressure Schur complement type[11], and the combination with parallel high performance computing techniques.

The next step regarding the benchmark will be the specification of how to submit and to collect the results. Moreover, it is planned to prepare a web page for collecting and presenting the FSI results. Then, based on the collected results, quantitative ratings regarding the main questions, particularly w.r.t. the coupling mechanisms and monolithic vs. partitioned approaches, might get possible.

**FSI2**: x & y displacement of the point $A$

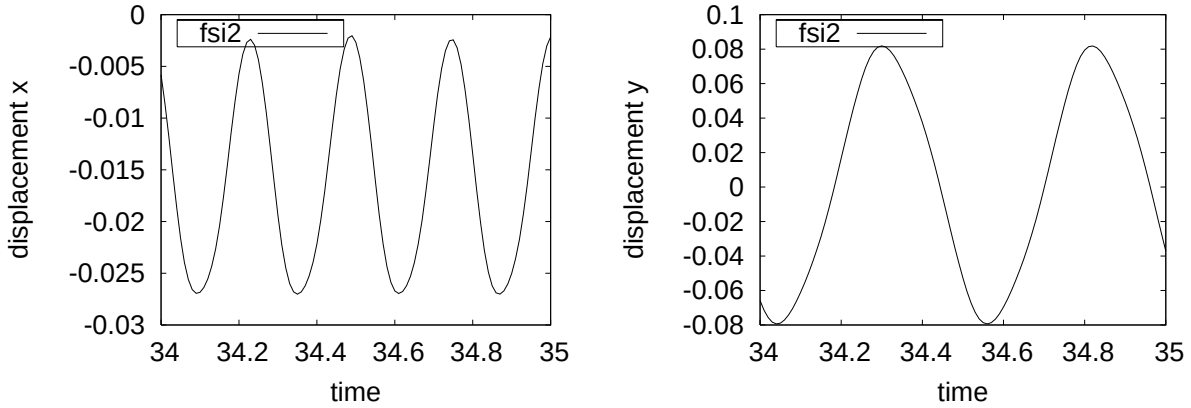


**FSI2**: lift and drag force on the cylinder+flag

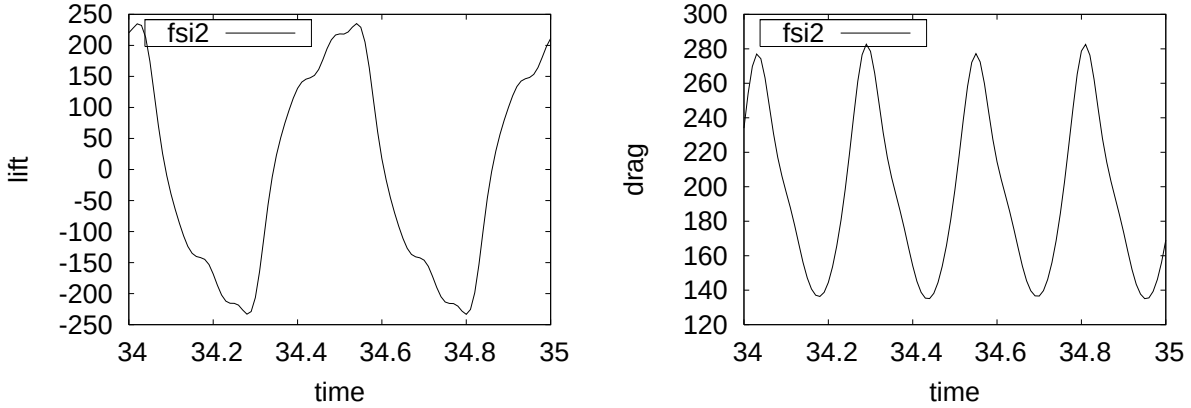


| lev. | ux of A $[\times 10^{-3}]$ | uy of A $[\times 10^{-3}]$ | drag | lift |
|---|---|---|---|---|
| 2 | $-14.00 \pm 12.03[3.8]$ | $1.18 \pm 78.7[2.0]$ | $209.46 \pm 72.30[3.8]$ | $-1.18 \pm 269.6[2.0]$ |
| 3 | $-14.25 \pm 12.03[3.8]$ | $1.20 \pm 79.2[2.0]$ | $202.55 \pm 67.02[3.8]$ | $0.71 \pm 227.1[2.0]$ |
| 4 | $-14.58 \pm 12.37[3.8]$ | $1.25 \pm 80.7[2.0]$ | $201.29 \pm 67.61[3.8]$ | $0.97 \pm 233.2[2.0]$ |
| lev. | ux of A $[\times 10^{-3}]$ | uy of A $[\times 10^{-3}]$ | drag | lift |
| 2 | $-14.15 \pm 12.23[3.7]$ | $1.18 \pm 78.8[1.9]$ | $210.36 \pm 70.28[3.7]$ | $0.80 \pm 286.0[1.9]$ |
| 3 | $-13.97 \pm 12.01[3.8]$ | $1.25 \pm 79.3[2.0]$ | $203.54 \pm 68.43[3.8]$ | $0.41 \pm 229.3[2.0]$ |
| 4 | $-14.58 \pm 12.44[3.8]$ | $1.23 \pm 80.6[2.0]$ | $208.83 \pm 73.75[3.8]$ | $0.88 \pm 234.2[2.0]$ |
| **ref.** | $-14.58 \pm 12.44[3.8]$ | $1.23 \pm 80.6[2.0]$ | $208.83 \pm 73.75[3.8]$ | $0.88 \pm 234.2[2.0]$ |

Figure 7: Results for **FSI2** with time step $\Delta t = 0.002, \Delta t = 0.001$

**FSI3**: x & y displacement of the point $A$

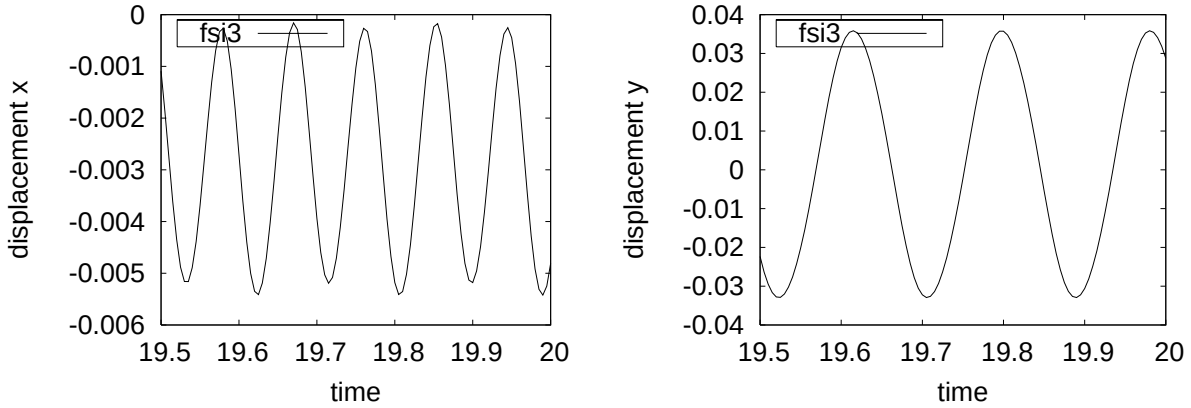


**FSI3**: lift and drag force on the cylinder+flag

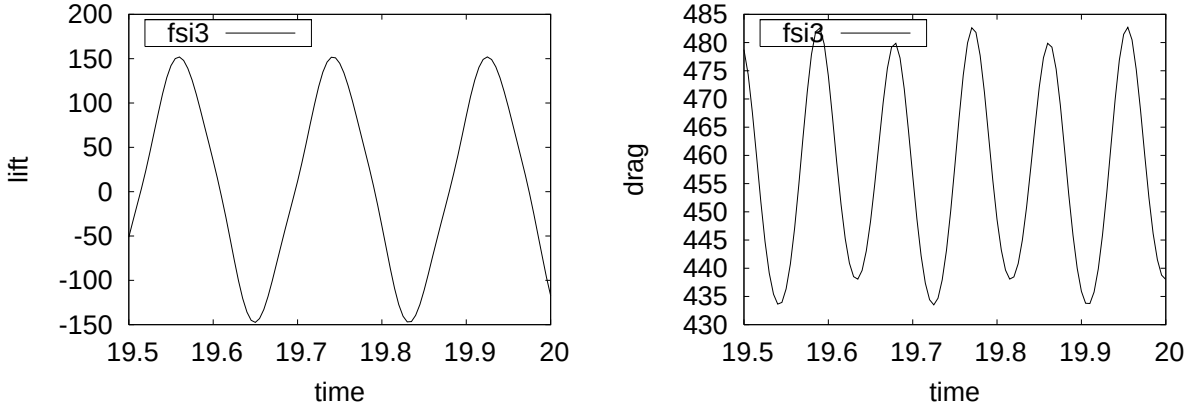


| lev. | ux of A $[\times 10^{-3}]$ | uy of A $[\times 10^{-3}]$ | drag | lift |
|---|---|---|---|---|
| 2 | $-3.02 \pm 2.78[10.6]$ | $0.99 \pm 35.70[5.3]$ | $444.6 \pm 31.69[10.6]$ | $9.48 \pm 151.55[5.3]$ |
| 3 | $-3.02 \pm 2.83[10.6]$ | $1.43 \pm 35.43[5.3]$ | $457.1 \pm 20.05[10.6]$ | $1.23 \pm 146.04[5.3]$ |
| 4 | $-2.85 \pm 2.56[10.9]$ | $1.53 \pm 34.35[5.3]$ | $459.8 \pm 20.00[10.9]$ | $1.51 \pm 148.76[5.3]$ |

| lev. | ux of A $[\times 10^{-3}]$ | uy of A $[\times 10^{-3}]$ | drag | lift |
|---|---|---|---|---|
| 2 | $-3.00 \pm 2.79[10.7]$ | $1.19 \pm 35.72[5.3]$ | $445.0 \pm 35.09[10.7]$ | $8.26 \pm 163.72[5.3]$ |
| 3 | $-2.86 \pm 2.68[10.7]$ | $1.45 \pm 35.34[5.3]$ | $455.7 \pm 24.69[10.7]$ | $1.42 \pm 146.43[5.3]$ |
| 4 | $-2.69 \pm 2.53[10.9]$ | $1.48 \pm 34.38[5.3]$ | $457.3 \pm 22.66[10.9]$ | $2.22 \pm 149.78[5.3]$ |
| **ref.** | $-2.69 \pm 2.53[10.9]$ | $1.48 \pm 34.38[5.3]$ | $457.3 \pm 22.66[10.9]$ | $2.22 \pm 149.78[5.3]$ |

Figure 8: Results for **FSI3** with time step $\Delta t = 0.001, \Delta t = 0.0005$

## REFERENCES

[1] R. Barrett, M. Berry, T. F. Chan, J. Demmel, J. Donato, J. Dongarra, V. Eijkhout, R. Pozo, C. Romine, and H. Van der Vorst. *Templates for the solution of linear systems: Building blocks for iterative methods*. SIAM, Philadelphia, PA, second edition, 1994.

[2] R. Bramley and X. Wang. *SPLIB: A library of iterative methods for sparse linear systems*. Department of Computer Science, Indiana University, Bloomington, IN, 1997. `http://www.cs.indiana.edu/ftp/bramley/splib.tar.gz`.

[3] T. A. Davis and I. S. Duff. A combined unifrontal/multifrontal method for unsymmetric sparse matrices. *ACM Trans. Math. Software*, 25(1):1–19, 1999.

[4] Charbel Farhat, Michel Lesoinne, and Nathan Maman. Mixed explicit/implicit time integration of coupled aeroelastic problems: three-field formulation, geometric conservation and distributed solution. *Int. J. Numer. Methods Fluids*, 21(10):807–835, 1995. Finite element methods in large-scale computational fluid dynamics (Tokyo, 1994).

[5] J. Hron and S. Turek. A monolithic FEM/multigrid solver for ALE formulation of fluid structure interaction with application in biomechanics. In H.-J. Bungartz and M. Schäfer, editors, *Fluid-Structure Interaction: Modelling, Simulation, Optimisation*, LNCSE. Springer, 2006.

[6] Bruno Koobus and Charbel Farhat. Second-order time-accurate and geometrically conservative implicit schemes for flow computations on unstructured dynamic meshes. *Comput. Methods Appl. Mech. Engrg.*, 170(1-2):103–129, 1999.

[7] Patrick Le Tallec and Salouna Mani. Numerical analysis of a linearised fluid-structure interaction problem. *Num. Math.*, 87(2):317–354, 2000.

[8] K. D. Paulsen, M. I. Miga, F. E. Kennedy, P. J. Hoopes, A. Hartov, and D. W. Roberts. A computational model for tracking subsurface tissue deformation during stereotactic neurosurgery. *IEEE Transactions on Biomedical Engineering*, 46(2):213–225, 1999.

[9] M. Rumpf. On equilibria in the interaction of fluids and elastic solids. In *Theory of the Navier-Stokes equations*, pages 136–158. World Sci. Publishing, River Edge, NJ, 1998.

[10] P. A. Sackinger, P. R. Schunk, and R. R. Rao. A Newton-Raphson pseudo-solid domain mapping technique for free and moving boundary problems: a finite element implementation. *J. Comput. Phys.*, 125(1):83–103, 1996.

[11] S. Turek. *Efficient solvers for incompressible flow problems: An algorithmic and computational approach*. Springer, 1999.

[12] S. Turek and J. Hron. Proposal for numerical benchmarking of fluid-structure interaction between an elastic object and laminar incompressible flow. In H.-J. Bungartz and M. Schäfer, editors, *Fluid-Structure Interaction: Modelling, Simulation, Optimisation*, LNCSE. Springer, 2006.

[13] S. Turek and M. Schäfer. Benchmark computations of laminar flow around cylinder. In E.H. Hirschel, editor, *Flow Simulation with High-Performance Computers II*, volume 52 of *Notes on Numerical Fluid Mechanics*. Vieweg, 1996. co. F. Durst, E. Krause, R. Rannacher.

[14] S.P. Vanka. Implicit multigrid solutions of Navier-Stokes equations in primitive variables. *J. of Comp. Phys.*, (65):138–158, 1985.